

Systematic study of the hidden order in URu₂Si₂ as a multipolar order; the role of triakontadipoles

Oscar Grånäs, Francesco Cricchio, and Lars Nordström

Department of Physics and Astronomy, Uppsala University, Box 516, SE-75120 Uppsala, Sweden

(Dated: March 9, 2022)

A systematic search for possible order parameters of the so-called hidden order of URu₂Si₂ is conducted. Among the possible candidates that do fulfill the experimental symmetry restrictions on the hidden order parameter, we find one candidate that stand out – one of the components of a triakontadipole multipole tensor that belongs to the A_{1u} irreducible representation of the point group D_{4h} . This solution is characterized by a $\vec{Q} = (0,0,1)$ ordering of the triakontadipoles and has a symmetry that forbids magnetic moments as well as most other multipole ordering on the uranium sites. This hidden order phase is closely related to the the antiferromagnetic phase, which is manifested in the similarities of the geometries of the calculated Fermi surfaces. Finally is found that this non-magnetic solution allows for another secondary superimposed order parameter that belong to B_{2u} , which gives rise to an anisotropic in-plane susceptibility without breaking the tetragonal crystal symmetry.

The hidden order (HO) of the heavy fermion material URu₂Si₂ has attracted a lot of interest since its discovery in 1985 [1], as described in a recent review [2]. The main enigma is at 17 K there is clear signature of a secondary phase transition but not of any observable order parameter (OP) in the HO phase. The only signal is that there is a tiny staggered magnetic moment which cannot account for the change in entropy at the phase transition. Another important aspect of the HO is that it under pressure goes through a phase transition to an anti-ferromagnetic (AF) phase with relatively large moments. This phase transition is now conclusively established to be of first order [3]. This and the fact that the order parameter of the HO phase does not cause any change in observable symmetries, such as crystal symmetry or magnetic moments, put some severe conditions on its symmetry properties.

There are numerous theoretical suggestions for the HO parameter in the literature, see Ref. [2] for a fuller account of these. Some are explicitly itinerant in nature as e.g. unconventional density waves [4], orbital currents [5], or helicity order [6]. Other focus more on the local atomic order parameter. In fact all multipolar order up to rank five have been suggested; quadrupoles [4], octupoles [8], hexadecapoles [9] and triakontadipoles [10].

In this Letter we will allow for a general real space atomic order parameter that can arise due to ordering of the itinerant uranium f -states. First we systematically study what symmetries of the OP that are consistent with various experimental observations. Then we test which of the OP candidates can be stabilized in a realistic calculations of the correlated f -electrons by means of a combined density functional theory and correlation treatment (DFT+ U). These complementary studies point towards which OP are allowed by symmetry and compatible with the electronic structure of URu₂Si₂. This study point conclusively towards an OP which is a superposition of two triakontadipole components belonging to different irreducible representations of the isogonal point group: $A_{1u} \oplus B_{2u}$.

We will allow for a staggered OP as a superposition of several independent OP, where each OP takes a general form

$$\psi^\alpha(\vec{Q}) = \frac{1}{N} \sum_n^N e^{i\vec{Q} \cdot \vec{R}_n} \langle f_n^\dagger \Gamma^\alpha f_n \rangle, \quad (1)$$

where \vec{Q} is an ordering wave vector, \vec{R}_n are the uranium atomic positions, N the number of atoms in the crystal, f_n^\dagger is the f -electron creation operator at atom site n and Γ^α is the operator for the local multipole of type α . Here Γ^α is a matrix-operator in the 14-dimensional space of f -orbitals and f_n is a vector-operator in the same space.

In order to have Eq. (4) to include all possible OP stemming from the f -shell, α should enumerate all possible degree of freedom within this shell. This is known to be handled by the so-called tesseral multipole tensor moments (TMTM) [1–3, 7, 10, 12], with $\alpha = \{kpr; t\}$,

$$w_t^{kpr}(n) = \text{Tr} \Gamma_t^{kpr} \langle f_n f_n^\dagger \rangle = \langle f_n^\dagger \Gamma_t^{kpr} f_n \rangle, \quad (2)$$

where the corresponding expansion matrices Γ_t^{kpr} are known matrices in the f -orbital space, see also *Supplementary Materials* (SM) [16] for more details. The multipole tensors in Eq. (5) have a simple physical interpretation; for even k , they are multipoles of the charge ($p=0$) or spin-magnetization ($p=1$), while for odd k they are multipoles of the corresponding currents. The rank of the tensor is given by r and its time reversal (TR) symmetry is given by $(-)^{k+p}$.

TABLE I: The TMTM components that corresponds to IR of the group D_{4h} . In the enumeration of the components t , $n \geq 0$ is an integer. The experimental compatibility for HO OP belonging to different IR of D_{4h} are ranked from the discussion points $i-iv$. Plus (minus) sign means that it has some (dis-) advantageous features for TR-even (g) and TR-odd (u) IR, respectively. For point iii there is the possibility of superimposed OP and the different letters indicate without any ranking order which two IR have to contribute together.

D_{4h}	character		even r	odd r	Hidden order	
IR	c_4	c_2	t	t	g	u
A_1	1	1	$+4n$	$-4(n+1)$	$++a-$	$++b+$
A_2	1	-1	$-4(n+1)$	$+4n$	$++c+$	$+-d-$
B_1	-1	1	$+2(2n+1)$	$-2(2n+1)$	$++c-$	$++d-$
B_2	-1	-1	$-2(2n+1)$	$+2(2n+1)$	$++a-$	$++b-$
E	0	0	$\pm(2n+1)$	$\pm(2n+1)$	$-++-$	$--+-$

It is easy to show that TMTM have simple transformations rules under point group operations. For a rotation with an angle ϕ around its quantization axis c and for a rotation by π around the first perpendicular direction a they behave as

$$\begin{aligned}\mathcal{R}(\hat{c}, \phi) w_t^{kpr}(n) &= \cos(t\phi) w_t^{kpr}(n) + \sin(t\phi) w_{-t}^{kpr}(n) \\ \mathcal{R}(\hat{a}, \pi) w_t^{kpr}(n) &= (-)^{t+r} \text{sgn}(t) w_t^{kpr}(n),\end{aligned}\quad (3)$$

respectively. In Table I the irreducible representations (IR) of the TMTM are determined for the tetragonal crystal point group D_{4h} through the characters of its two generators, $c_4 = \mathcal{R}(\hat{c}, \pi/2)$ and $c_2 = \mathcal{R}(\hat{a}, \pi)$, where a and c denote the lattice directions.

Before we present our calculations we will reinvestigate which of the TMTM OP that are compatible with the most important constraints put on the HO OP that have been gathered by the huge amount of experimental studies. It is not possible to cover all experimental aspects [2], so we concentrate on experimental observations that have simple and direct implication on the symmetry aspects of the HO.

i) **Non-broken lattice symmetry.** At high temperatures URu_2Si_2 has the crystal symmetry of the space group 139 (I4/mmm) with its isogonal point group D_{4h} (4/mmm). It is established that there are no lattice distortions at the HO transition at 17 K, i.e. the HO phase also belong to the tetragonal crystal class. Since the uranium atoms are situated at maximally symmetric Wyckoff sites the local site symmetry is also D_{4h} . Then from Table I it is clear that if the local four-fold rotation remains, the OP has to belong to the A_1 or A_2 IR of the point group. However when the crystal symmetries are taken into account one can see that the broken local four-fold symmetry can be taken care of by crystal symmetry operations, which has been noted earlier for the case of quadrupoles [18]. The remedy is a four-fold screw axis generated by the non-symmorphic symmetry operation $(c_4|\frac{1}{2}\frac{1}{2}\frac{1}{2})$. In the cases of B_1 and B_2 IR the tetragonal symmetry is recovered for an ordering wave vector $\vec{Q} = (001)$, while for E the corresponding wave vector is $(00\frac{1}{2})$.

ii) **Vanishing magnetic moments.** Since it is now established that the phase transition under pressure from the HO phase to the AF phase is of first order [3], the HO OP cannot belong to A_{2u} since it is the IR of magnetic moments along the c -axis. If we are looking for a symmetry reason for the non-existence of magnetic moments in the HO phase, the IR of the HO OP cannot neither belong to E_u , the IR of the in-plane magnetic moments.

iii) **Low symmetry in-plane susceptibility.** Recently there have been reported that the HO phase has a broken four-fold symmetry [5]. An analysis has shown that this arises from the OP squared that interacts with the applied magnetic field squared, which leads to a non-vanishing B_{2g} IR of the magnetic susceptibility [6, 16]. In Ref. [6] it was shown that only the OP belonging to E has a B_{2g} IR in the direct product representation of its square, $B_{2g} \in E_\nu \otimes E_\nu$, $\nu = \{g, u\}$.

Another option is that OP is a linear combination of two independent OP of different IR. Then since [16] $A_{1\nu} \otimes B_{2\nu} = A_{2\nu} \otimes B_{1\nu} = B_{2g}$, we see that the co-existence of these type of OP would also lead to the observed variation of the magnetic susceptibility. Note that the two OP have to have the same TR symmetry ν , i.e. even or odd.

iv) **Good hideout.** From Table I we can observe that even when the primary OP would have a high rank which makes it hard to observe directly, it will leave traces in terms of induced multipoles of lower ranks. In that sense there are two type of OP that have the chance to be better hidden than others. They are OP with $t = -4$ and either even $r \geq 4$ belonging to IR A_2 or with odd $r \geq 5$ belonging to IR A_1 .

Summary of candidates. Our survey is summarized in Table I. It is a linear combination of OP that best fulfill the criteria from point $i-iv$, either $A_{1u} \oplus B_{2u}$ or $A_{2g} \oplus B_{1g}$, while the best pure OP belongs to either A_{1u} or A_{2g} .

Electronic structure calculations. In order to determine which of the TMTM are compatible with the electronic structure, we will perform a systematic survey in terms of realistic calculations. Care has to be taken to allow for TMTM OP solutions as of Eq. (4) that belong to the different IR of the isogonal group D_{4h} as listed in Table I. In our approach we break the symmetry by inducing staggered w_t^{kpr} on the uranium sites and determine the largest possible symmetry group that is compatible with their existence. Then by iteration we determine if this starting assumption converges to a non-trivial solution. In principle it is possible that two cases of induced OP of the same IR do lead to two different solutions, but they may of course also converge to the same solution.

The electronic structure is determined with the DFT+ U approximation within the APW+ lo method as implemented in the ELK-code [8, 9]. The calculations were performed in a similar way as earlier described [2, 7, 10], and is presented in more details in SM [16].

For each possible TMTM component of each IR as given in Table I we have started a calculation with a large value of the corresponding multipole. All calculations enforce a staggering wave vector $\vec{Q} = (001)$ for tensors with rank $r \geq 1$. It was found that one solution exists for each TR-labelled IR and these results are collected in Table II for the case of $U = 1$ eV. In order to quantify the importance of different tensor components we have utilized the concept of polarization π_t^{kpr} [7], which is a normalization independent quantity that directly measures the importance of the different contributions to the polarization of the density matrix. It is proportional to the square of the components of the TMTM w_t^{kpr} and all components except $kpr = 000$ add up to a total polarization π^{tot} , see SM [16] for more details.

In the case of TR-even all IR converged to the trivial un-polarized case of A_{1g} with only the rotational invariant tensors, w_0^{000} and w_0^{110} , being non-zero. They correspond to expectation values of the f -occupation and the operator $\ell \cdot s$, respectively. The calculated large value of w_0^{110} leads to an enhancement of the intrinsic spin-orbit coupling, which brings the solution in to a relativistic regime with predominantly $j = 5/2$ occupation. The resulting OP is not actually staggered.

When the TR symmetry is broken we find in all cases that components of the triakontadipole w_t^{615} dominate. In addition we find smaller contributions from all TMTM components that are allowed by symmetry as given in Table I, that is both TR-odd as well as TR-even. However, only two TMTM have significant polarizations, w_0^{110} and w_t^{615} for all cases except A_{2u} and E_u . In all these cases the w_0^{110} have similar polarizations as in the TR-even case.

The case of A_{2u} is the most complicated. Here there is a strong competition for the exchange energy between the magnetic dipole moments along c -axis and the two allowed triakontadipole components. The magnetic dipoles have significant polarization for all three MP variants, spin w_0^{011} , orbital w_0^{101} , and spin dipolar w_0^{211} , while the triakontadipole w_0^{615} has a contribution of similar strength but w_4^{615} has the largest polarization. Although all initializations lead to the same solution, the convergence is often extremely slow which indicates that there is a flat energy-landscape. This was observed in the earlier study where we first observed the triakontadipoles in the A_{2u} phase [10]. For the two dimensional IR E_u we have performed two calculations where the OP is oriented along the in-plane symmetry directions (100) and (110), respectively. Both the two solutions are stable although different, indicating a strong anisotropy. As anticipated both cases possess non-vanishing magnetic moments. The local magnetic moments are 1.1 and 0.8 μ_B , respectively. No polarized solution could be found in the case of tetragonal E_u , i.e. with the ordering vector $\vec{Q}/2$.

For the TR-odd case we have also looked for the possibility of superimposed OP. Only one new solution was found when allowing for various combinations of superimposed OP, but this is one of the HO OP candidates that were singled out fulfilling all the experimental constraints. It is $A_{1u} \oplus B_{2u}$, with the $\psi_{-4}^{615}(\vec{Q})$ two orders of magnitude larger than $\psi_2^{615}(\vec{Q})$. The product of these two OP interacts with the global magnetic field in the ab -plane and gives rise to a nonzero B_{2g} IR of the magnetic susceptibility [16], which explains the in-plane response of the torque experiments [5].

In Fig. 1 the variation of the Fermi surface (FS) sheets are displayed, from the uncorrelated cases to the finite $U = 0.5$ eV and 1.0 eV cases for both the two solutions with largest polarizations, the A_{1u} and A_{2u} . At $U = 0$ they reproduce the FS of Ref. [26]. A_{2u} corresponds to their AF solution, and the, in this case unpolarized, A_{1u} corresponds to their paramagnetic. In this limit, we observe that the FS of the two solutions are radically different, while at finite U they become surprisingly similar. Hence if we would identify the non-magnetic solution with a A_{1u} OP as the HO phase and the magnetic solution A_{2u} as the AF phase, we see that the calculated FS are in excellent qualitative accordance with recent Shubnikov-de Haas measurements [27] that observe only minor changes in the phase transition from HO to AF phase under pressure. In the calculated case we can see very large resemblances in topology as well as sizes between the FS of the two solutions at both $U = 0.5$ eV and $U = 1$ eV. Since the FS for the two different U -values do not even have the same topology, the FS geometry is very U dependent. So it is left for a future study to calculate more in detail the U variation of the FS and to compare more quantitatively with experiments.

TABLE II: The different solutions for calculations with $U = 1$ eV. For each IR label, the total polarization, the dominating ($\pi_t^{\text{kpr}} \geq 1$) TMTM components, their values and their polarizations are given. For E_u the case with largest polarization, which is with the two independent components along the plane diagonal (110), is presented.

IR	π^{tot}	kpr	t	w_t^{kpr}	π_t^{kpr}
A_{1g}	4.8	110	0	-2.5	4.8
A_{1u}	12.8	615	-4	44.9	7.0
A_{2u}	14.6	011	0	1.0	1.0
		101	0	-0.8	1.3
		615	4	-36.5	4.7
B_{1u}	12.2	615	-2	39.7	5.5
B_{2u}	11.9	615	2	39.6	5.5
E_u (110)	14.5	615	± 5	-24.2	2.0
		615	± 1	20.3	1.4
$A_{1u} \oplus B_{2u}$	12.8	615	-4	44.9	7.0
		615	2	0.5	$7 \cdot 10^{-4}$

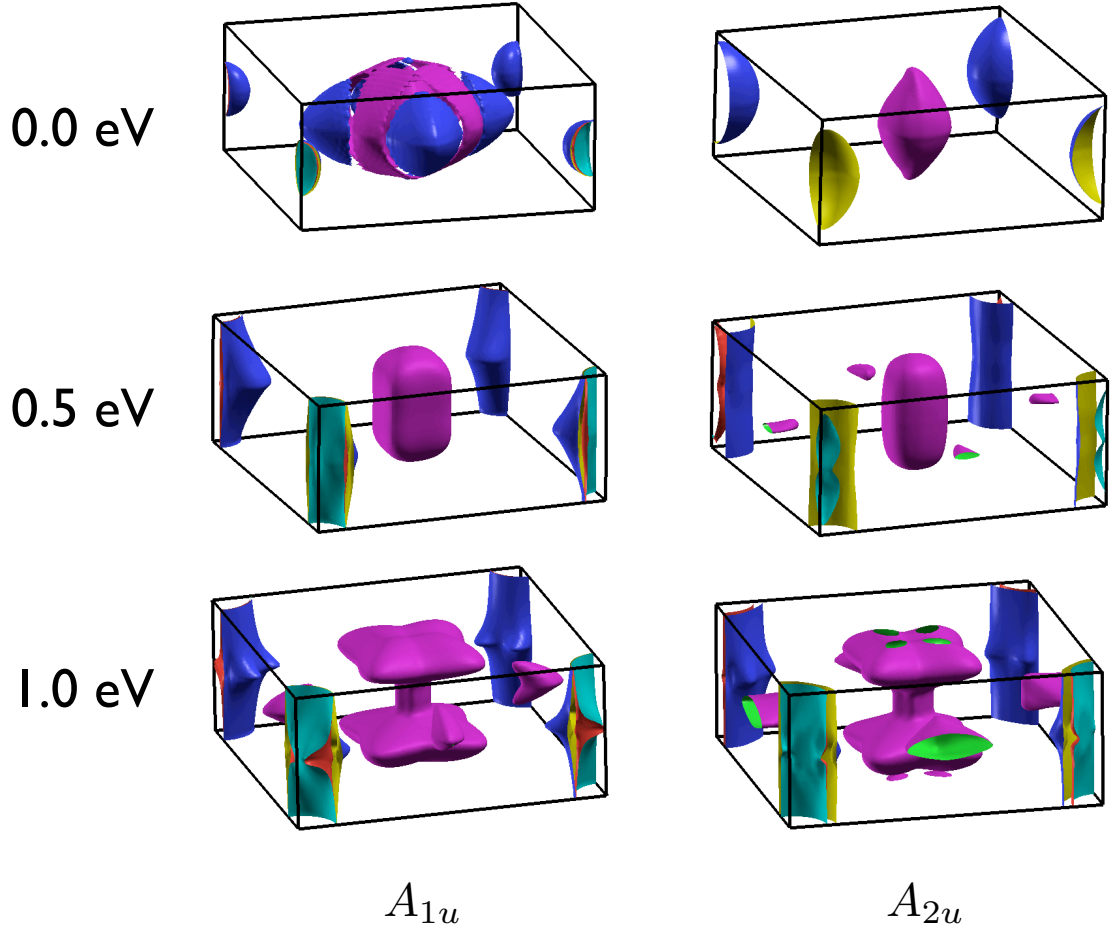


FIG. 1: The Fermi surface of URu_2Si_2 as a function of parameter U for the case of OP belonging to the IR A_{1u} and A_{2u} , respectively. The green/purple, blue/yellow and red/light-blue colors on the different sides of the Fermi sheets refer to the electron/hole side.

In this study we have performed a detailed and systematic survey of possible HO OP in terms of ordering within the uranium f -bands. A picture arises from some common features of Tables I and II. First we observe there are no indication at all in the calculations for a TR-even HO OP. Secondly, it is clear that the AF solution at high pressure is the IR A_{2u} where the OP in the calculation is a superposition of magnetic vector OP and TR-odd rank 5 TMTM components, with the last ones dominating. Thirdly, this phase competes with an almost pure TMTM OP of the kind $\psi_{-4}^{615}(\vec{Q})$ which belong to the IR A_{1u} . These two solutions, A_{2u} and A_{1u} , are among the ones that have the largest polarizations, as shown in Table II. The HO phase A_{1u} only allows a few multipolar components with tesseral component $t = -4$, where all except w_{-4}^{615} become small. This leads to an optimally hidden OP. It is further found that there exist a solution where this A_{1u} OP is superimposed with a smaller B_{2u} triakontadipole OP, which would explain the recently observed anisotropic in-plane susceptibility[5].

From Table II we can directly observe that the various solutions for the different IR all have a large contribution from the rank 5 TMTM OP ψ^{615} . These results are in good accordance with our earlier observations that these trikontadipoles play a large role for URu₂Si₂ in particular [10] and for the time reversal symmetry breaking for moderate or strong spin-orbit coupling in general [7]. The latter is summarized as Katts' rules. After completion of this study we became aware of a recent calculational study [28] which also identify the importance of large rank 5 multipoles in the electronic structure of URu₂Si₂. In those random phase approximation (RPA) calculations only the $j = 5/2$ states are included (see [16] for a discussion) and it was concluded that the magnetic $r = 5 E_u$ state is the best candidate for the HO phase.

The support from the Swedish Research Council (VR) is thankfully acknowledged. The calculations have been performed at the Swedish high performance centers HPC2N and NSC under grants provided by the Swedish National Infrastructure for Computing (SNIC).

-
- [1] T.T.M. Palstra, A.A. Menovsky, J. van den Berg, A.J. Dirkmaat, P.H. Kes, G.J. Nieuwenhuys and J.A. Mydosh, Phys. Rev. Lett. **55**, 2727 (1985).
 - [2] J.A. Mydosh and P.M. Oppeneer, Rev. Mod. Phys. **83**, 1301 (2011).
 - [3] P.G. Niklowitz, C. Peiderer, T. Keller, M. Vojta, Y.-K. Huang, and J.A. Mydosh, Phys. Rev. Lett. **104**, 106406 (2010).
 - [4] H. Ikeda and Y. Ohashi, Phys. Rev. Lett. **81**, 3723 (1998).
 - [5] P. Chandra, P. Coleman, J.A. Mydosh and V. Tripathi, Nature (London) **417**, 831 (2002).
 - [6] C. M. Varma and L. Zhu, Phys. Rev. Lett. **96**, 036405 (2006).
 - [7] P. Santini and G. Amoretti, Phys. Rev. Lett. **73**, 1027 (1994).
 - [8] A. Kiss and P. Fazekas, Phys. Rev. B **71**, 054415 (2005).
 - [9] K. Haule and G. Kotliar, Nature Phys. **5**, 796 (2009).
 - [10] F. Cricchio, F. Bultmark, O. Grånäs and L. Nordström, Phys. Rev. Lett. **103**, 107202 (2009).
 - [11] G. van der Laan and B.T. Thole, J. Phys.: Condens. Matter **7**, 9947 (1995).
 - [12] G. van der Laan, Phys. Rev. B **57**, 112 (1998).
 - [13] F. Bultmark, F. Cricchio, O. Grånäs and L. Nordström, Phys. Rev. B **80**, 035121 (2009).
 - [14] F. Cricchio, F. Bultmark and L. Nordström, Phys. Rev. B **78**, 100404 (2008).
 - [15] F. Cricchio, O. Grånäs and L. Nordström, Europhys. Lett. **94**, 57009 (2011).
 - [16] O. Grånäs, F. Cricchio and L. Nordström, Supplementary Materials.
 - [17] P. Thalmeier and T. Takimoto, Phys. Rev. B **83**, 165110 (2011).
 - [18] H. Harima, K. Miyake, and J. Flouquet, J. Phys. Soc. Jpn **79**, 033705 (2010).
 - [19] E. Hassinger, G. Knebel, K. Izawa, P. Lejay, B. Salce, and J. Flouquet, Phys. Rev. B **77**, 115117 (2008).
 - [20] P.A. Sharma, N. Harrison, M. Jaime, Y.S. Oh, K.H. Kim, C.D. Batista, H. Amitsuka, and J.A. Mydosh, Phys. Rev. Lett. **97**, 156401 (2006).
 - [21] M. Nakashima, H. Ohkuni, Y. Inada, R. Settai, Y. Haga, E. Yamamoto, and Y. Onuki, J. Phys.: Condens. Matter **15**, S2011 (2003).
 - [22] Y.J. Jo, L. Balicas, C. Capan, K. Behnia, P. Lejay, J. Flouquet, J.A. Mydosh and P. Schlottmann, Phys. Rev. Lett. **98**, 166404 (2007).
 - [23] R. Okazaki, T. Shibauchi, H. J. Shi, Y. Haga, T. D. Matsuda, E. Yamamoto, Y. Onuki, H. Ikeda, and Y. Matsuda, Science **331**, 439 (2011).
 - [24] D. Singh and L. Nordström Planewaves, Pseudopotentials, and the LAPW method, Springer Verlag, New York, (2006).
 - [25] ELK an all-electron open source full-potential augmented plane wave plus local orbitals (APW+*lo*) code, that is available at <http://elk.sourceforge.net>.
 - [26] S. Elgazzar, J. Ruzs, M. Amft, P.M. Oppeneer and J.A. Mydosh, Nature Mater. **8**, 337 (2009).
 - [27] E. Hassinger, G. Knebel, T. D. Matsuda, D. Aoki, V. Taufour and J. Flouquet, Phys. Rev. Lett. **105**, 216409 (2010).
 - [28] H. Ikeda, M.-T. Suzuki, R. Arita, T. Takimoto, T. Shibauchi and Y. Matsuda, Nature Phys. **8**, 528 (2012).

SUPPLEMENTARY MATERIALS

ORDER PARAMETERS

In this study our main focus is on order parameters (OP) of the general form

$$\begin{aligned}\psi_t^{kpr}(\vec{Q}) &= \frac{1}{N} \sum_n^N e^{i\vec{Q} \cdot \vec{R}_n} \langle f_n^\dagger \Gamma_t^{kpr} f_n \rangle \\ &= \frac{1}{N} \sum_n^N e^{i\vec{Q} \cdot \vec{R}_n} w_t^{kpr}(n),\end{aligned}\quad (4)$$

where \vec{Q} is an ordering wave vector, \vec{R}_n are the uranium atomic positions, N the number of atoms in the crystal and f_n^\dagger is the f -electron creation operator at atom site n . Γ_t^{kpr} is the operator for the local tesseral multipole tensor moment (TMTM) component,

$$w_t^{kpr}(n) = \text{Tr} \Gamma_t^{kpr} \rho_n = \text{Tr} \Gamma_t^{kpr} \langle f_n f_n^\dagger \rangle = \langle f_n^\dagger \Gamma_t^{kpr} f_n \rangle, \quad (5)$$

where the trace is over the f orbitals. For a f -shell $0 \leq k \leq 6$, $0 \leq p \leq 1$ and $|k-p| \leq r \leq k+p$, which constitute 26 different multipole tensors, of which 13 are time reversal (TR) even and 13 TR-odd, and the total number of tensor components are $196 = 14 \times 14$. This then accounts for the full freedom of the 14-dimensional density matrix $\rho_n = \langle f_n f_n^\dagger \rangle$. In the 14-dimensional space of f -orbitals, Γ_t^{kpr} is a matrix-operator and f_n is a vector-operator. In a $\{jm_j\}$ -representation of the f -states (jj -basis) we have

$$\Gamma_{t,12}^{kpr} = \frac{\sqrt{[j_1 j_2]}}{N_{kpr\ell}} (-)^{k+p+r} \begin{Bmatrix} \ell & \ell & k \\ s & s & p \\ j_1 & j_2 & r \end{Bmatrix} \gamma_{t,m_1 m_2}^{j_1 j_2 r} \quad (6)$$

$$\gamma_{t,m_1 m_2}^{j_1 j_2 r} = (-)^{j_1 - m_1} \mathcal{T} \begin{pmatrix} j_1 & r & j_2 \\ -m_1 & t & m_2 \end{pmatrix}. \quad (7)$$

Here $\ell = 3$, $s = 1/2$, the (\dots) - and $\{\dots\}$ -symbols are the Wigner-3j and -9j, respectively, $N_{kpr\ell}$ is a normalization factor and $[a\dots b] = (2a+1)\dots(2b+1)$. [1, 2] The operator \mathcal{T} brings a spherical tensor, which was used in earlier studies [2, 3], to a tesseral form

$$\mathcal{T}a_t = \begin{cases} [a_t + (-)^t a_{-t}] / \sqrt{2} = \sqrt{2} \Re a_t & t > 0 \\ a_t & t = 0 \\ i[a_t - (-)^t a_{-t}] / \sqrt{2} = \sqrt{2} \Im a_{|t|} & t < 0 \end{cases}. \quad (8)$$

The tesseral form is convenient when considering rotational symmetries as in the present study. The TMTM in Eq. (4) have a simple physical interpretation; for even k , they are multipoles of the charge ($p=0$) or spin-magnetization ($p=1$), while for odd k they are multipoles of the corresponding currents. The rank of the tensor is given by r and its time reversal (TR) symmetry is given by $(-)^{k+p}$.

Hence all possible OP stemming from the f -shell is covered by a superposition of OP in terms of TMTM of Eq. 4. For instance the OP of an ordinary spin density wave is given by $\psi_t^{011}(\vec{Q})$. This can be easily seen since $\Gamma_t^{011} = \tilde{\sigma}_t$, the Pauli spin matrices in tesseral form, i.e. $\tilde{\sigma}_1 = \sigma_x$, $\tilde{\sigma}_{-1} = \sigma_y$ and $\tilde{\sigma}_0 = \sigma_z$, respectively. Another example is $\psi_2^{112}(\vec{Q})$, which is one of the staggered quadrupoles models suggested in Ref. 4.

Symmetry properties

It is easy to show that TMTM have simple transformations rules under point group operations. For a rotation with an angle ϕ around its quantization axis (which we denote z) and for a rotation by π around the first perpendicular direction (which we denote x) they behave as

$$\begin{aligned}\mathcal{R}(\hat{z}, \phi) w_t^{kpr}(n) &= \cos(t\phi) w_t^{kpr}(n) + \sin(t\phi) w_{-t}^{kpr}(n) \\ \mathcal{R}(\hat{x}, \pi) w_t^{kpr}(n) &= (-)^{t+r} \text{sgn}(t) w_t^{kpr}(n),\end{aligned}\quad (9)$$

respectively. Hence the rotational properties are determined by the rank r and the component t only. In Table I of the main Letter (ML) the irreducible representations (IR) of the TMTM are determined for the isogonal point group D_{4h} through the characters of its two generators, $c_4 = \mathcal{R}(\hat{c}, \pi/2)$ and $c_2 = \mathcal{R}(\hat{a}, \pi)$. In addition the TMTM behave under a TR-operation Θ as

$$\Theta w_t^{kpr}(n) = (-)^{k+r} w_t^{kpr}(n). \quad (10)$$

As the local site group for the uranium atoms is equal to the isogonal point group, Table ML-I describes the local symmetry for the different IR. Then it is clear that only A_1 and A_2 are compatible with the fourfold rotational symmetry of the tetragonal space group. However, this symmetry is recovered also for the other IR if super-cells are allowed for. This comes from the non-symmorphic group element $(c_4 | \frac{1}{2} \frac{1}{2} \frac{1}{2})$, a fourfold screw operation that connects the corner (n even) and body-centered (n odd) uranium sites in the original bct structure. It maintains the tetragonal symmetry also for the other IR, as for B_1 and B_2 we get

$$\left(c_4 | \frac{1}{2} \frac{1}{2} \frac{1}{2} \right) w_{\pm 2}^{kpr}(0) = -w_{\pm 2}^{kpr}(1) \quad (11)$$

$$\left(c_4 | \frac{1}{2} \frac{1}{2} \frac{1}{2} \right)^2 w_{\pm 2}^{kpr}(0) = w_{\pm 2}^{kpr}(2) \quad (12)$$

while for E we get (q is an integer $0 \leq q \leq (r-1)/2$)

$$\left(c_4 | \frac{1}{2} \frac{1}{2} \frac{1}{2} \right) w_{[q]}^{kpr}(0) = w_{-[q]}^{kpr}(1) \quad (13)$$

$$\left(c_4 | \frac{1}{2} \frac{1}{2} \frac{1}{2} \right)^2 w_{[q]}^{kpr}(0) = -w_{[q]}^{kpr}(2) \quad (14)$$

$$\left(c_4 | \frac{1}{2} \frac{1}{2} \frac{1}{2} \right)^3 w_{[q]}^{kpr}(0) = -w_{-[q]}^{kpr}(3) \quad (15)$$

$$\left(c_4 | \frac{1}{2} \frac{1}{2} \frac{1}{2} \right)^4 w_{[q]}^{kpr}(0) = w_{[q]}^{kpr}(4). \quad (16)$$

where for odd $t = [q] = 2q + 1$, w_t^{kpr} and w_{-t}^{kpr} span the two-dimensional IR. The operations leading to a change of sign of the TMTM, i.e. Eqs. (11) and (14), correspond to ordering vectors $\vec{Q} = (001)$ and $\vec{Q}/2$, respectively.

Susceptibility

As discussed in the ML there are no experimental signature that the tetragonal crystal symmetry is broken in the hidden order (HO) phase. However, recently in measurements of the in-plane susceptibility on single URu₂Si₂ crystals an anisotropic component was detected. [5] This was subsequently analyzed by Thalmeier and Thakimoto [6]. Here we will extend their analysis and show that the experiments can be explained by a non-vanishing B_{2g} contribution to the in-plane susceptibility. The experiments are based on measurements of the torque on the sample in a uniform external magnetic field H that are constrained to the ab plane of the tetragonal crystal. This torque is given by

$$\vec{\tau} = \mu_B V \chi \vec{H} \times \vec{H}, \quad (17)$$

where V is the sample volume, χ the susceptibility tensor and $\vec{H} = (H_a, H_b, 0) = H(\cos \phi, \sin \phi, 0)$. The in-plane part of the symmetric χ tensor is decomposed into three IR

$$\mathcal{Rep}[\chi_{\parallel}] = A_{1g} \oplus B_{1g} \oplus B_{2g} = \mathcal{Rep}[\chi_{aa} + \chi_{bb}] \oplus \mathcal{Rep}[\chi_{aa} - \chi_{bb}] \oplus \mathcal{Rep}[\chi_{ab}]. \quad (18)$$

Then the torque is given by

$$\vec{\tau} = \mu_B V H^2 \hat{c} \left\{ \frac{1}{2} (\chi_{aa} - \chi_{bb}) \sin 2\phi - \chi_{ab} \cos 2\phi \right\}, \quad (19)$$

i.e. with two-fold symmetric contributions from the B_{1g} and B_{2g} IR of the susceptibility, respectively.

TABLE III: The IR decomposition of the direct product of two IR: the factors given by the row and column and the direct product in their intersection. ν labels the TR symmetry, either even g or odd u .

D_{4h}	$A_{1\nu}$	$A_{2\nu}$	$B_{1\nu}$	$B_{2\nu}$	E_ν
$A_{1\nu}$	A_{1g}	A_{2g}	B_{1g}	B_{2g}	E_g
$A_{2\nu}$	A_{2g}	A_{1g}	B_{2g}	B_{1g}	E_g
$B_{1\nu}$	B_{1g}	B_{2g}	A_{1g}	A_{2g}	E_g
$B_{2\nu}$	B_{2g}	B_{1g}	A_{2g}	A_{1g}	E_g
E_ν	E_g	E_g	E_g	E_g	$A_{1g} \oplus A_{2g} \oplus B_{1g} \oplus B_{2g}$

Furthermore, these susceptibilities will have contributions from the HO, $\Psi(\vec{Q})$, through its interaction with the magnetic field in the Landau free energy expansion

$$\begin{aligned}\mathcal{F}_H &= g_1[\Psi(\vec{Q})^2]_{B_{1g}}[\vec{H}^2]_{B_{1g}} + g_2[\Psi(\vec{Q})^2]_{B_{2g}}[\vec{H}^2]_{B_{2g}} + \dots \\ &= g_1[\Psi(\vec{Q})^2]_{B_{1g}} \frac{1}{2}(H_a^2 - H_b^2) + g_2[\Psi(\vec{Q})^2]_{B_{2g}} H_a H_b + \dots,\end{aligned}\quad (20)$$

where only second order interactions appear due to the staggering of the HO, $\vec{Q} \neq 0$, while the magnetic field is uniform. Thus the B_{1g} susceptibility are proportional to $[\Psi(\vec{Q})^2]_{B_{1g}}$, i.e. the B_{1g} part of the IR decomposition of the squared OP, while the B_{2g} susceptibility are proportional to $[\Psi(\vec{Q})^2]_{B_{2g}}$, since by definition $\chi_{ij} = \partial^2 \mathcal{F} / \partial H_i \partial H_j$. From Table III one can see that there are three ways each to get B_{1g} and B_{2g} contributions in the IR decomposition of a squared OP, i.e. $\mathcal{R}ep[\Psi(\vec{Q})] \otimes \mathcal{R}ep[\Psi(\vec{Q})]$. B_{1g} can be obtained from $A_{1\nu} \otimes B_{1\nu}$, $A_{2\nu} \otimes B_{2\nu}$ or $E_\nu \otimes E_\nu$, while B_{2g} can be obtained from $A_{1\nu} \otimes B_{2\nu}$, $A_{2\nu} \otimes B_{1\nu}$ or $E_\nu \otimes E_\nu$, where ν indicates the TR symmetry, even (g) or odd (u).

In the torque measurements [5] a $\cos 2\phi$ oscillation was observed in the HO phase only, which imply that there is a non-vanishing χ_{ab} , i.e. a B_{2g} IR, in the presence of the HO OP. Hence, if this OP belongs to a single IR of the point group D_{4h} , only $\mathcal{R}ep[\Psi(\vec{Q})] = \Psi_{E_\nu}(\vec{Q})$ gives rise to the observed two-fold in-plane susceptibility χ_{ab} , i.e. only OP of IR E_g or E_u are candidates for the HO. On the other hand if the OP is a superposition of components belonging to different IR, OP of type $\mathcal{R}ep[\Psi(\vec{Q})] = \Psi_{A_{2\nu}}(\vec{Q}) \oplus \Psi_{B_{1\nu}}(\vec{Q}) \oplus \dots$ or $\mathcal{R}ep[\Psi(\vec{Q})] = \Psi_{A_{1\nu}}(\vec{Q}) \oplus \Psi_{B_{2\nu}}(\vec{Q}) \oplus \dots$ are also possible. Hence in a general case, with an OP having contributions from all possible IR, we have that

$$\chi_{ab} = \frac{\partial^2 \mathcal{F}}{\partial H_a \partial H_b} = \sum_\nu 2g_2 (\Psi_{A_{1\nu}} \Psi_{B_{2\nu}} + \Psi_{A_{2\nu}} \Psi_{B_{1\nu}} + \Psi_{E_{\nu a}} \Psi_{E_{\nu b}}). \quad (21)$$

Here $\Psi_{E_{\nu a}}$ and $\Psi_{E_{\nu b}}$ span the two-dimensional IR E_ν and are chosen such that $c_4 E_{\nu a} = E_{\nu b}$, $c_2 E_{\nu a} = (-)^{r+1} E_{\nu a}$ and $c_2 E_{\nu b} = (-)^r E_{\nu a}$, with r the rank of the OP tensor.

Relativistic effects

In presence of strong spin-orbit coupling, there will be a large splitting between the $j = \ell - 1/2 = 5/2$ and $j = \ell + 1/2 = 7/2$ states. Then it is useful to study the density matrix in a jj -basis

$$\rho_n = \begin{pmatrix} \rho_n^{\frac{5}{2} \frac{5}{2}} & \rho_n^{\frac{5}{2} \frac{7}{2}} \\ \rho_n^{\frac{7}{2} \frac{5}{2}} & \rho_n^{\frac{7}{2} \frac{7}{2}} \end{pmatrix},$$

where each sub-matrix $\rho_n^{j_1 j_2}$ is spanned by m_1 and m_2 with $-j_1 < m_1 < j_1$ and $-j_2 < m_2 < j_2$.

Strong spin-orbit coupling

Let us first discuss the limit of very strong spin-orbit coupling. In this limit the TMTM w_0^{110} is related to w_0^{000} through $w_0^{110} = -\frac{4}{3} w_0^{000}$, and only the $j = 5/2$ occupation is non-zero. As we well discuss below, URu₂Si₂ does not fulfill this criterion and hence rather possess an intermediately strong spin-orbit coupling. However it is interesting to study this limit not least since it is assumed in some other theoretical studies. In this relativistic limit the $j = 7/2$

states are much higher in energy than the $j = 5/2$ states and the occupation is restricted to the sub-matrix $\rho_n^{\frac{5}{2}\frac{5}{2}}$ of Eq. (22). In this limit the TMTM are then given by

$$w_t^{kpr}(n) \approx \text{Tr} \Gamma_t^{kpr} \rho_n^{\frac{5}{2}\frac{5}{2}} \quad (22)$$

$$= \frac{6}{N_{kpr\ell}} (-)^{k+p+r} \left\{ \begin{matrix} \ell & \ell & k \\ s & s & p \\ 5/2 & 5/2 & r \end{matrix} \right\} \sum_{m_1 m_2} \gamma_{t, m_1 m_2}^{\frac{5}{2}\frac{5}{2}r} \rho_{n, m_2 m_1}^{\frac{5}{2}\frac{5}{2}}. \quad (23)$$

Now from the definition of γ_t^{jjr} in Eq. (7), one can see that r in Eq. (23) is given by the vector coupling of two $j = 5/2$ angular momenta, and hence can take values in between 0 and 5. From general relations for exchange of two columns in the $9j$ symbols

$$\left\{ \begin{matrix} \ell & \ell & k \\ s & s & p \\ j & j & r \end{matrix} \right\} = (-)^{2\ell+2s+2j+k+p+r} \left\{ \begin{matrix} \ell & \ell & k \\ s & s & p \\ j & j & r \end{matrix} \right\}. \quad (24)$$

Now the fact that $2(\ell + s + j)$ is always even the $9j$ -symbol in Eq. (23) has to be zero for odd $k + p + r$. Hence only even $k + p + r$ TMTM contribute in this limit. This in turn gives that odd (even) r multipolar moments have to be TR-odd (TR-even).

The different rank r TMTM are then related through Eq. (23), e.g. in the case of $r = 5$ the TMTM with $kpr = 505$, 415 and 615 have fixed ratios of

$$\frac{w_t^{415}}{w_t^{615}} = \frac{N_{615}}{N_{415}} \frac{\left\{ \begin{matrix} 3 & 3 & 4 \\ 1/2 & 1/2 & 1 \\ 5/2 & 5/2 & 5 \end{matrix} \right\}}{\left\{ \begin{matrix} 3 & 3 & 6 \\ 1/2 & 1/2 & 1 \\ 5/2 & 5/2 & 5 \end{matrix} \right\}} \approx 0.013 \quad (25)$$

$$\frac{w_t^{505}}{w_t^{615}} = \frac{N_{615}}{N_{505}} \frac{\left\{ \begin{matrix} 3 & 3 & 5 \\ 1/2 & 1/2 & 0 \\ 5/2 & 5/2 & 5 \end{matrix} \right\}}{\left\{ \begin{matrix} 3 & 3 & 6 \\ 1/2 & 1/2 & 1 \\ 5/2 & 5/2 & 5 \end{matrix} \right\}} \approx -0.077. \quad (26)$$

In this case the 615 TMTM is largest which is just an example of the general case. The spin dependent ($p = 1$) TMTM have largest weight for the $r = k - 1$ tensor moments, as these are favored by the spin-orbit coupling for less than half-filled f -shell.

Intermediately strong spin-orbit coupling

For a full f -shell the TMTM OP with highest rank is the $\psi_t^{617}(\vec{Q})$ of rank 7 and in this case the TR symmetry is not given by rank r , as also odd $k + p + r$ TMTM are allowed. They are included in all the analysis for completeness, although these tensor moments are somewhat obscure. Within these the orbital and spin degrees of freedom couple in an axial way, as of e.g. $\mathbf{w}^{111} = \frac{2}{3}\vec{\ell} \times \vec{s}$. These tensor moments only arise from the off diagonal $j_1 \neq j_2$ blocks of Eq. (22) as they are not allowed in the block-diagonal part as the corresponding $9j$ -symbols have to vanish according to Eq. (24). They will be included in the analysis and it would be fascinating if they would play a role, but in the present case of URu₂Si₂ they are of marginal interest.

That URu₂Si₂ belongs to the case of intermediately strong spin-orbit coupling can be directly seen from the occupation numbers. Both the f -occupation, w_0^{000} , as well as the effective spin orbit coupling, w_0^{110} , are essentially independent on the assumed IR and take values around 2.6 and -2.5 , respectively. This corresponds to that w_0^{110} has

a value 70% of its saturation value, $-\frac{4}{3}w_0^{000}$. The occupation number for the 5/2 sub-shell is then given by

$$n_{5/2} = \frac{3}{7}w_0^{000} - \frac{3}{7}w_0^{110} \approx 2.2, \quad (27)$$

while for the 7/2 it is

$$n_{7/2} = \frac{4}{7}w_0^{000} + \frac{3}{7}w_0^{110} \approx 0.4. \quad (28)$$

The extra flexibility of having a non-zero $n_{7/2}$ can lead to a stronger 615-polarization on the expense of the 415 and 505 ones. This is e.g. confirmed in that the calculated ratios corresponding to Eqs. (25) and (26) are 0.006 and -0.052 , respectively, for the case of A_{1u} and $t = -4$.

Polarization

In order to quantify the importance of different tensor components we have utilized the concept of polarization [7], π_t^{kpr} is a normalization independent quantity that directly measures the importance of the different contributions to the polarization of the density matrix. It is proportional to the square of the components of the TMTM w_t^{kpr} and all components except $kpr = 000$ For each tensor component except, $k = p = r = 0$,

$$\pi_t^{kpr} = [\ell skpr] |N_{kpr\ell} w_t^{kpr}|^2, \quad (29)$$

which all add up to a total polarization $\pi^{\text{tot}} = \sum_{kprt} \pi_t^{kpr}$. The total polarization is constrained by the inequality $\pi^{\text{tot}} \leq nn_h$, where n is the occupation number of the f -shell and n_h the corresponding number of holes.

ELECTRONIC STRUCTURE CALCULATIONS

In ML a systematic study which of the TMTM are compatible with the electronic structure were conducted through realistic calculations.

The electronic structure was determined with the DFT+ U approximation within the APW+ lo method as implemented in the ELK-code. [8, 9] In the DFT+ U approach a screened Hartree-Fock interaction is included among the 5 f states only. The Slater parameters $F^{(k)}$ are determined individually by using a screened Yukawa potential, this approach has been showed to be particularly convenient since all four $F^{(k)}$ are controlled by the choice of a single parameter, the parameter U . [2] For double-counting we adopt the automatic interpolation scheme of Pethukov *et al.* [10] The calculations were performed at the experimental lattice constants. [1] The muffin-tin radius R_{MT}^U of U is set to 1.9 Å, and those of Ru and Si are set to 1.2 Å. The parameter $R_{\text{MT}}^U |\vec{G} + \vec{k}|_{\text{max}}$, governing the number of plane waves in the APW+ lo method, is chosen to be 9.5. To allow for the \vec{Q} order the unit cell is doubled and the corresponding Brillouin zone is sampled with $18 \times 18 \times 10$ k -points.

Care has to be taken to allow for TMTM OP solutions as of Eq. (4) that belong to the different IR of the isogonal group D_{4h} as listed in Table I of ML. In our approach we break the symmetry by inducing staggered w_t^{kpr} on the uranium sites and determine the largest possible symmetry group that is compatible with their existence. Then by iteration we determine if this starting assumption converges to a non-trivial solution.

-
- [1] G. van der Laan and B.T. Thole, J. Phys.: Condens. Matter **7**, 9947 (1995).
 - [2] F. Bultmark, F. Cricchio, O. Grånäs and L. Nordström, Phys. Rev. B **80**, 035121 (2009).
 - [3] F. Cricchio, F. Bultmark and L. Nordström, Phys. Rev. B **78**, 100404 (2008).
 - [4] P. Santini and G. Amoretti, Phys. Rev. Lett. **73**, 1027 (1994).
 - [5] R. Okazaki, T. Shibauchi, H. J. Shi, Y. Haga, T. D. Matsuda, E. Yamamoto, Y. Onuki, H. Ikeda, and Y. Matsuda, Science **331**, 439 (2011).
 - [6] P. Thalmeier and T. Takimoto, Phys. Rev. B **83**, 165110 (2011).
 - [7] F. Cricchio, O. Grånäs and L. Nordström, Europhys. Lett. **94**, 57009 (2011).
 - [8] D. Singh and L. Nordström Planewaves, Pseudopotentials, and the LAPW method, Springer Verlag, New York, (2006).
 - [9] Elk an all-electron open source full-potential augmented plane wave plus local orbitals (APW +lo) code, that is available at <http://elk.sourceforge.net>.
 - [10] A.G. Petukhov, I.I. Mazin, L. Chioncel and A.I. Lichtenstein, Phys. Rev. B **67**, 153106 (2003).